Effect of size on the Coulomb staircase phenomenon in metal nanocrystals

P. John Thomas, G.U. Kulkarni, C.N.R. Rao *

Chemistry and Physics of Materials Unit, Jawaharlal Nehru Centre for Advanced Scientific Research, Jakkur P.O., Bangalore-560-064, India

Received 8 February 2000; in final form 2 March 2000

Abstract

The Coulomb staircase in polymer-covered Pd and Au nanocrystals of varying diameters in the 1.7–6.4 nm has been investigated by employing tunneling conductance measurements. Charging up to several electrons is observed at room temperature in the I–V data. Small nanocrystals show charging steps exceeding 200 mV while the larger ones exhibit smaller steps. Significantly, the charging energies follow a scaling law of the form, $U = A + B/d$, where d is the diameter of the nanocrystal. Furthermore, the line widths in the derivative spectra also vary inversely with the diameter. © 2000 Published by Elsevier Science B.V. All rights reserved.

1. Introduction

Single-electron circuits promise possible alternatives to semiconductor based integrated circuits, information storage devices, infrared radiation receivers and so on [1]. Averin and Likharev [2] first proposed the concept of single-electron tunneling in the absence of a Josephson junction. A manifestation of single-electron tunneling is the Coulomb staircase behavior observed in the I–V characteristics of tunnel junctions with capacitances of the order of a few aF $(10^{-18}$ F). Fig. 1 illustrates how it is realized using tunneling spectroscopy. The tunnel junction incorporates a tiny capacitor in the form of a ligated metal nanocrystal. Charging of the nanocrystal occurs in increments of single electrons, giving rise to

a series of equally spaced steps in the I–V spectrum (Fig. 1b). Andres et al. [3] observed such a staircase with a gold nanocrystal of 3 nm diameter deposited in vacuum on a layer of self-assembled molecules. Metal nanocrystals prepared by the wet-chemical methods have also been found to exhibit the staircase phenomenon [4,5]. Chen et al. [6] have studied ensembles of mass selected gold particles covered with alkane thiols using differential pulse voltametry while Petit et al. [7] observed Coulomb charging effects in ferromagnetic monolayers of Co nanoparticles.

To our knowledge, there has been no investigation of the effect of particle size in the Coulomb staircase phenomenon in isolated metal nanocrystals. In this Letter, we report the results of our study of the Coulomb staircase in Au and Pd nanocrystals of varying sizes (1.7–6.4 nm), protected by polyvinylpyrrolidone (PVP). In this range, the nanocrystals are small enough to have discrete charg-

---

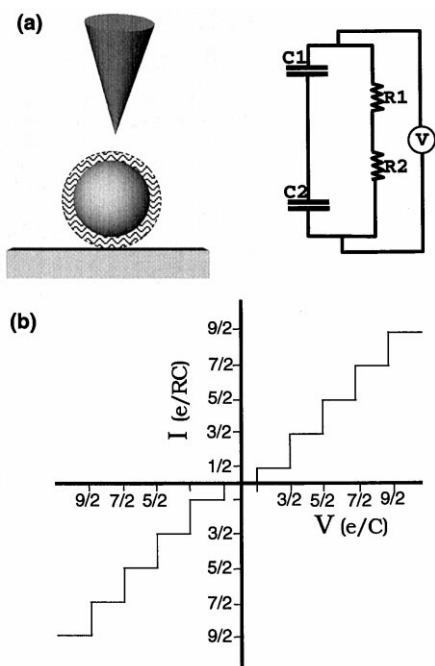* Corresponding author. Fax: +91-80-846-2766; e-mail: cnrrao@jncasr.ac.in

Fig. 1. Schematic illustration of (a) a single-electron tunnel junction formed by a nanocrystal held between the STM tip and the substrate. The particle diameter varies between 1.7 and 6.4 nm and the thickness of the PVP coating is ~ 1 nm. The 'equivalent' circuit is shown alongside. (b) I–V data showing a Coulomb staircase.

ing energies but are above the non-metallic regime [8,9]. The present study brings out several interesting aspects of the Coulomb staircase phenomenon. Specially noteworthy is our finding that the charging energy estimated from the staircases follow a scaling law.

2. Experimental

Nanocrystals of Pd and Au dispersed in the form of metal sols were obtained by wet chemical methods. The Pd sols were prepared by the reduction of the salts using ethanol. In order to obtain monodispersed Pd_{561} nanocrystals, the procedure of Miyake et al. [10] was followed. Accordingly, a 15 ml of 2.0 mM aqueous solution of H_2PdCl_4 was reduced with a mixture of 15 ml of absolute ethanol and 25 ml of water in the presence of 33.3 mg PVP (M_w, 40 000 gmol^{-1}). Although one cannot entirely be certain

that the Pd nanocrystals obtained by this procedure contained exactly 561 atoms in the five-shell closed configuration, there is little doubt that the particles were monodispersed with a uniform diameter of 2.5 nm as evidenced by transmission electron microscopy (JEOL 3010-TEM, 300 kV). Imaging at high resolution showed the icosahedral shape of the particle and confirmed its crystalline nature [11]. A Pd sol containing bigger particles was obtained by a growth process starting with the Pd_{561} sol. Equal volumes of Pd_{561} sol and 0.6 mM H_2PdCl_4 in ethanol–water (2:3) were refluxed for 1 h which yielded particles of diameter, ~ 4.5 nm. Yet another Pd sol was prepared by reducing 33.5 mg of $Pd(OAc)_2$ with ethanol (125 ml) in the presence of 190 mg of PVP [12]. A mean particle diameter of ~ 6.0 nm was obtained in this case. The size distributions in the last two sols were somewhat broader compared to that of the Pd_{561} sol. Au nanocrystals of different diameters were obtained from a single sol prepared by the photoreduction method [13]. A 15 ml sample of 0.5 mM solution of $HAuCl_4$ in formamide containing 2 mM of PVP was irradiated with UV light from a mercury vapor lamp (60 W) for 3 h. The irradiation increased the overall temperature of the precursor by $\sim 10°C$ when the color changed from orange-red to pale violet. TEM images showed that the Au sol contained particles in the 1.5–12 nm range with the mean at ~ 8 nm.

Tunneling conductance measurements were performed using a Nanoscope-II (Digital instruments, USA), operating at room temperature in air. A high impedance of 2.5 MΩ (bias, 500 mV; set-point current, 2 nA) was used for imaging to prevent tip induced damage and capture of the metal particle by the tip. The microscope was initially calibrated against the (0001) surface of highly oriented pyrolytic graphite (HOPG) using an Au tip prepared by electrochemical means [14]. The same tip was used throughout the course of the study. Prior to tunneling measurements, the Pd sols were recrystallized from diethyl ether in order to remove excess ions. The Au sols required no further purification [13]. Samples were prepared by depositing a few drops of the dilute metal sol on a freshly cleaved HOPG and allowing it to dry in vacuum. STM imaging of the sols showed the presence of well separated particles on the graphite surface, although the mean diameters

were somewhat higher than those from TEM mea-surements [15]. For instance, the diameter of the Pd_{561} nanocrystal was 3.3 nm as compared to 2.5 nm in the TEM. This gave a rough estimate for the thickness of the ligand shell to be ∼ 0.8 nm. Such estimates could not be obtained for other nanocrys-tals because of wider size distributions. The diameter values referred to hereafter are from the STM mea-surements.

I–V data were collected in the spectroscopy mode with the feedback loop turned off. Initially, large areas typically 200 nm^2 were scanned to locate isolated nanocrystals such that any possibility of interference from the neighbors in the I–V measure-ment could be ruled out. After obtaining a stable, non-drifting image of an isolated nanocrystal, 200 I–V data points were collected in a typical voltage sweep of ±750 mV across zero, with a delay of 100 µS between successive sweeps. The I data points were then normalized with respect to the set-point current. Imaging of the area was repeated after the I–V measurement to ensure that the nanocrystal had not drifted away. We have carried out measurements under the same conditions of bias and current (500 mV, 2 nA) on the various Pd and Au nanocrystals.

3. Results and discussion

In Fig. 2 we show the I–V data obtained with Pd nanocrystals of 3.3, 4.4 and 6.4 nm diameter. The curves are characteristic of metal − insulator − metal (MIM) junctions [16], modulated on either side of the zero bias by a series of current–voltage steps. The 3.3 nm nanocrystal, corresponding to Pd_{561} ex-hibits a step width of 208 mV or a charging energy of 208 meV. The voltage range studied (±750 mV) was wide enough to allow charging of the nanocrys-tal up to several electrons. What is striking is that both the step width and the number of steps vary with the nanocrystal diameter. The step width, which is 208 mV for the 3.3 nm nanocrystal, decreases to 158 mV in the case of the 4.4 nm nanocrystal, and to 116 mV with that having 6.4 nm diameter. The 3.3 nm nanocrystal exhibits three steps on either side of the zero bias which amounts to three times the
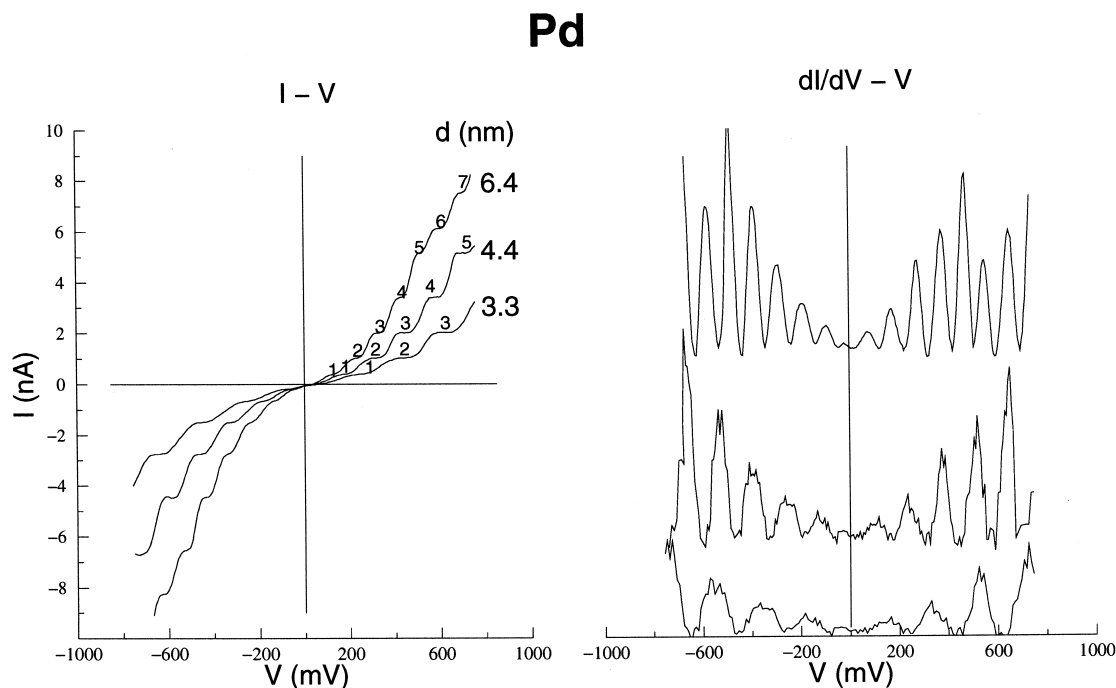

Fig. 2. I–V data of isolated Pd nanocrystals of different sizes. The derivative spectra are shown alongside.

electronic charge on it. The 4.4 and 6.4 nm nanocrystals display five and seven steps, respectively in the same voltage range. We also notice that the overall current is higher for the larger metal cores [8]. The derivative spectra shown in Fig. 2 reveal uniformly spaced peaks corresponding to the steps in the I–V data.

We have treated the I–V data using a semiclassical model [17] based on a double junction of capacitors. According to the model, the observed capacitance (C) may be resolved into two components C_1 and C_2, and the resistance (R) into R_1 and R_2, such that $C = C_1 + C_2$ and $R = R_1 + R_2$ (see Fig. 1a). For $C_1 \ll C_2$ and $R_1 \ll R_2$, the model predicts steps in the measured current to occur at critical voltages,

$$V_c = n_c e / C + (1/C)(q_0 + e/2) \tag{1}$$

where q_0 is the residual charge. The fit obtained in the case of the 3.3 nm Pd nanocrystal is shown in Fig. 3. We see noticeable deviations from the model especially at higher voltages. Considering that the measurements were carried out at room temperature, it is noteworthy that the semiclassical model is in reasonable agreement with the data. The analysis gave estimates for the circuit constants as follows:
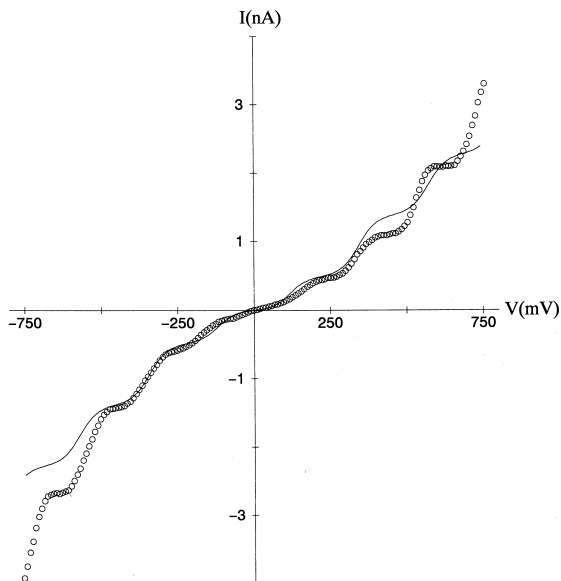

Fig. 3. I–V characteristic of an isolated 3.3 nm Pd nanocrystal (dotted line) and the theoretical fit (solid line) obtained with the semiclassical model for T = 300 K.

$C_1 = 0.07$ aF, $C_2 = 0.7$ aF, $R_1 = 0.5$ MΩ, $R_2 = 255$ MΩ, $q_0 = 0e$. These values are typical of ligated metal clusters [17]. The classical expression for the capacitance of a metal sphere in a dielectric medium is [18],

$$C_d = 2\pi\varepsilon_0\varepsilon d. \tag{2}$$

Here d is the diameter of the particle. Assuming $\varepsilon_{PVP} = 3$ [13], we obtain $C_{3.3nm} \sim 0.6$ aF which matches closely with the tunneling measurement. Similar results were obtained with other nanocrystals.

The I–V data obtained with the Au nanocrystals are shown in Fig. 4. The smallest nanocrystal studied (1.7 nm) exhibits a three-step Coulomb staircase each with a width of 229 mV. Larger nanocrystals display a larger number of steps with smaller widths, just as the Pd nanocrystals. The MIM characteristics in Fig. 4 are somewhat distorted especially in the case of smaller nanocrystals, possibly due to an unfavorable ratios of the capacitances and resistances [5].

In order to examine whether the charging energies obtained from the above data follow a scaling law of the form,

$$U = A + B/d, \tag{3}$$

we have plotted the charging energy against $1/d$ in Fig. 5. We see that the plots are linear showing that the scaling law is indeed obeyed. The intercepts for the Pd and Au nanocrystals are quite close (17 and 40 meV, respectively). The slopes (B) are, however, different 627 and 318 meV nm^{-1}, respectively. Such a scaling law proposed with respect to free metal clusters, on the basis of theoretical considerations [19], predicts a significantly higher value of the slope (1440 meV nm^{-1}). The difference may be due to the presence of the polymer coating and also possibly due to interaction with the substrate. The values of the intercepts are related to the bulk inner band energies [19].

An interesting observation from the derivative spectra in Figs. 2 and 4 is that the line width, which is a representation of the diffused nature of a Coulomb step, varies with the nanocrystal size. The line width for the 3.3 nm Pd nanocrystal is ~ 107 mV while for 4.4 and 6.4 nm nanocrystals, the widths are 72 and 38 mV, respectively. A similar
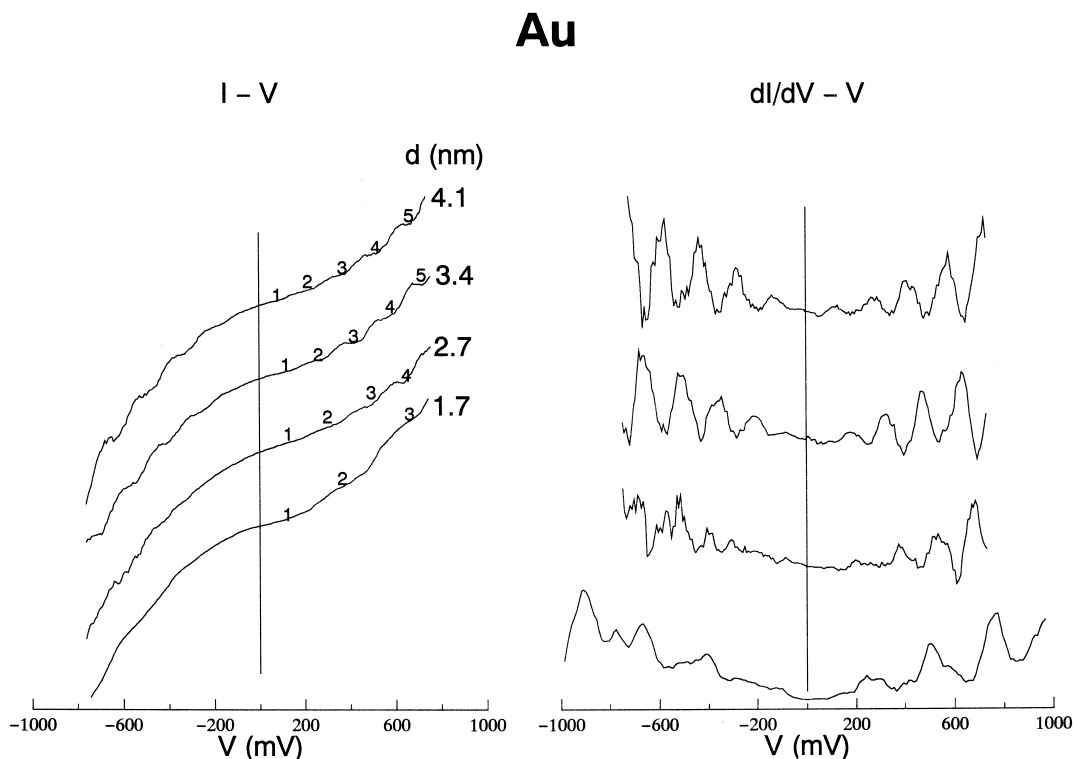
Au

Fig. 4. I–V data of isolated Au nanocrystals of different sizes. The derivative spectra are shown alongside.

trend is seen in the case of Au nanocrystals (Fig. 4). It is possible that such smearing of the I–V data occurs due to thermal excitations in the tunnel junc-
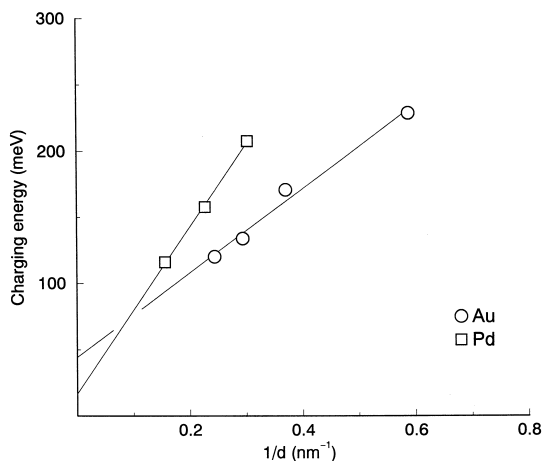

Fig. 5. Variation of the charging energies of Pd and Au nanocrystals with inverse diameter (d).

tion at room temperature. However, the observed systematics do point to a size effect. It is noteworthy that the line width also exhibits a linear relationship with the inverse diameter, much like the charging energy itself. The two systems of nanocrystals exhibit different slopes and intercepts. We do not have an explanation for the size dependence of the line width at this stage. It is possible that the observed line broadening could arise due to tunneling from the vicinity of the Fermi level of the nanocrystal to the substrate, the tunnel barrier decreasing with decreasing nanocrystal size [20]. This effect could also arise, in principle, due to an off-centered tip. We, however, believe this not to be the case in the present study.

In conclusion, we have observed the Coulomb staircase phenomenon at room temperature in tunnel junctions formed by PVP ligated nanocrystals of Pd and Au. Our observations clearly relate to the charging effects of a classical conducting particle, the charging energy obeying a scaling law with respect to the inverse of the diameter. The observed differences in charging energies of Au and Pd nanoparti-

cles may originate from the inherent differences in the electronic structure of Pd and Au systems (viz., $5d^{10}$ and $5d^{10}6s^1$, respectively). The interaction of the metal with the ligand shell should also be taken into account.

Acknowledgements

References

[1] D.V. Averin, K.K. Likharev, in: H. Grabert, M.H. Devoret (Eds.), Single Electron Tunneling, Plenum, New York, 1992, p. 311.

[2] D.V. Averin, K.K. Likharev, J. Low Temp. Phys. 62 (1986) 345.

[3] R.P. Andres, T. Bein, M. Dorogi, S. Feng, J.I. Henderson, C.P. Kubiak, W. Mahorey, R.G. Osifchin, R. Reifenber, Science 272 (1996) 1323.

[4] H. van Kempen, J.G.A. Dubois, J.W. Gerritsen, G. Schmid, Physica B 204 (1995) 51.

[5] J.G.A. Dubois, J.W. Gerritsen, S.E. Shafranjuk, E.J.G. Boon, G. Schmid, H. van Kempen, Europhys. Lett. 33 (1996) 279.

[6] S. Chen, R.S. Ingram, M.J. Hostetler, J.J. Pietron, R.W. Murray, T.G. Schaaf, J.T. Khoury, M.M. Alvarez, R.L. Whetten, Science 280 (1998) 2098.

[7] C. Petit, T. Cren, D. Roditchev, W. Sacks, J. Jlein, M.P. Pileni, Adv. Mater. 11 (1999) 1998.

[8] C.P. Vinod, G.U. Kulkarni, C.N.R. Rao, Chem. Phys. Lett. 289 (1998) 329.

[9] P.P. Edwards, R.L. Johnston, C.N.R. Rao, in: P. Braunstein, G. Oro, P.R. Raithby (Eds.), Metal Clusters in Chemistry, Wiley–VCH, 1999.

[10] T. Teranishi, M. Miyake, Chem. Mater. 10 (1998) 594.

[11] C.N.R. Rao, G.U. Kulkarni, P. John Thomas, P.P. Edwards, Chem. Soc. Rev. 29 (2000) 27.

[12] F. Porta, F. Ragaini, S. Cenini, Gazz. Chem. Ital. 122 (1992) 361.

[13] M.Y. Han, L. Zhow, C.H. Quek, S.F.Y. Li, N. Huang, Chem. Phys. Lett. 287 (1998) 47.

[14] A.J. Nam, A. Teren, J.A. Lusby, A.J. Melmed, J. Vac. Sci. Technol. B 115 (1996) 2046.

[15] M.T. Reetz, W. Helbig, S.A. Quaiser, U. Stimming, N. Breuer, R. Vogel, Science 276 (1995) 367.

[16] W.J. Kaiser, R.C. Jaklevic, IBM J. Res. Dev. 30 (1986) 4.

[17] M. Amman, R. Wilkins, E. Ben-Jacaob, P.D. Amker, R.C. Jaklevic, Phys. Rev. B 43 (1991) 1146.

[18] S. Carrara, in: J.H. Fendler (Ed.), Nanoparticles and Nanostructured Films, Wiley–VCH, New York, 1998, p. 349.

[19] J. Jortner, Z. Phys. D 24 (1992) 247.

[20] J. Jortner, Private communication.